This is a peer-reviewed, author's accepted manuscript of the following conference output:
Abdel-Aziz, A., Ahmed, K., Massoud, A., & Williams, B. (2022). A new torque ripple minimization approach for switched reluctance drives.
Paper presented at 1st IEEE Industrial Electronics Society Annual On-Line Conference (ONCON) 2022.

A New Torque Ripple Minimization Approach for Switched Reluctance Drives

Ali Abdel-Aziz
Department of Electronic and Electrical Engineering
University of Strathclyde
Glasgow, UK
ali.hassan-abdelaziz-ali@strath.ac.uk

Euan MacRae
Department of Electronic and Electrical Engineering
University of Strathclyde
Glasgow, UK
euan.macrae@strath.ac.uk

Neville McNeill
Department of Electronic and Electrical Engineering
University of Strathclyde
Glasgow, UK
neville.mcneill@strath.ac.uk

Khaled Ahmed
Department of Electronic and Electrical Engineering
University of Strathclyde
Glasgow, UK
khaled.ahmed@strath.ac.uk

Ahmed Massoud
Department of Electrical Engineering
Qatar University
Doha, Qatar
ahmed.massoud@qu.edu.qa

Barry Williams
Department of Electronic and Electrical Engineering
University of Strathclyde
Glasgow, UK
barry.williams@strath.ac.uk

***Abstract*—This paper presents a new torque control function for torque ripple reduction in switched reluctance drives. The approach is based on the maximum utilization of available dc link voltage, extending the zero torque-ripple speed range. The approach is suitable for switched reluctance machines with any number of phases and stator/rotor poles. Soft switching control is deployed, which reduces switching losses. At any instant, only one phase current is controlled, significantly reducing the control complexity. Simulations are carried out on a four-phase 8/6, 4kW SRM in MATLAB/Simulink.**

Keywords—Electric vehicles, switched reluctance motor, torque ripple minimization, torque sharing function.

I. INTRODUCTION

The switched reluctance machine (SRM) has many merits, such as robustness, simple construction, low cost, and no permanent magnets [1], [2]. However, its deployment in servo applications is restrained due to: firstly, acoustic noise caused by radial vibration [3], secondly severe torque ripple (TR) during commutation (the transfer of torque production from an outgoing phase to an incoming phase) due to the discrete and non-linear nature of SRM torque production [4], and thirdly non-standard converter bridge configuration [5]. The high torque ripple may cause mechanical vibration stresses (possibly resulting in mechanical resonance effects) and speed oscillation at low speeds, which are undesirable in applications such as the electric vehicle (EV) [6], [7]. Many solutions have been proposed to alleviate the first two undesirable SRM features [8].

Generally, two main approaches are available to reduce TR: the machine design approach and the control approach [9]. Modifying the machine design is limited to a narrow speed range and for rated load conditions. Moreover, changes to the basic rotor/stator design result in reduced power output, an unacceptable SRM limitation in EVs. As opposed to the machine design approach, the control approach is less expensive, more effective, and flexible, and can cover a wide range of speeds [10].

Among different control approaches, torque sharing functions (TSFs) reliably reduce the TR generated during commutation [11]. In [12], the objective was to optimize linear and sinusoidal TSFs to reduce TR along with phase rms current. However, saturation was neglected, and analytical expressions were required to optimize the process. In [13], the concept of maximum rate of change of flux linkage was introduced to assess conventional TSFs (linear, sinusoidal, cubic, and exponential). It was shown that a low rate of change of flux linkage increases the ripple-free speed range. In addition, optimal values for turn-on and overlap angles were advised.

A logical non-linear TSF was proposed in [14], with no attention to the maximum rate of change of flux linkage. In [15], an online TSF was proposed, where the selection between incoming and outgoing phases during commutation is determined based on the value of the rate of change of flux linkage. Nevertheless, this method requires a PI controller to compensate for the error between the reference and estimated torque. Also, converting the torque expression to the current expression requires an analytical formula.

An offline TSF was presented in [16], which offers a trade-off between low rms current and low rate of change of flux linkage. The model requires accurate analytical expressions to derive the current profiles. A direct instantaneous torque control (DITC) based TSF was proposed in [17], which requires fewer current sensors. However, the phase current detection accuracy is low. Also, circuit modification and two high-frequency pulse width modulation (PWM) signals are required for phase current extraction.

A hybrid switching mode (a combination of hard and soft switching) was proposed in [18] instead of the hard switching mode usually adopted in conventional TSFs.

However, there was no illustration of this method's maximum ripple-free speed range. In [19], an off-line TSF based on SRM magnetic characteristics was proposed, where a weighting parameter is adjusted to minimize the rms current, while ensuring that the rate of change of flux linkage is below the dc link voltage, for accurate current tracking. In [20], a TR minimization technique based on a non-linear modulating factor was proposed for a four-phase, 8/6 SRM, where TR is reduced by modifying the incoming phase current. However, the proposed technique requires modification to be implemented for SRMs with a different number of phases and stator/rotor poles. Moreover, the technique is based on mathematical modeling of the SRM, which is prone to inaccuracy due to severe SRM non-linearity.

In the literature, all TSFs have some salient shortcomings, which can be summarized as follows:

- The dc link voltage is not fully exploited, limiting the ripple-free speed range.
- Hard or hybrid switching is required for accurate current tracking, increasing switching losses.

This paper presents an offline torque control function (TCF, as opposed to a TSF, since torque will be controlled by only controlling one phase) based on SRM magnetic characteristics. The new TR analysis concept is introduced, separating torque ripple into two independent parts: phase commutation torque-ripple and switching (PWM/ hysteresis) torque ripple.

The merits of the proposed TCF are:

- The method is suitable for SRMs with any number of phases and stator/rotor pole numbers.
- Maximum utilization of available dc link voltage is achieved at turn-on and turn-off, with no switching.
- The SRM maximum speed range with theoretically zero TR (commutation ripple elimination, leaving ripple due to PWM switching only) is determined.
- Soft switching control is deployed (as opposed to hard or hybrid switching usually adopted for traditional TSFs), reducing switching losses.
- The proposed TCF requires switching for a period equal to the stroke angle instead of the full conduction period, reducing switching losses.
- At any instant (regardless of the number of phases conducting simultaneously), only one phase current is controlled, hence termed torque control function, TCF.

The paper is organized as follows: Section II presents the new off-line TCF with the proposed control technique. Section III investigates the maximum torque ripple-free speed range achieved at different torque demands using the proposed TCF. Simulation results are given in Section IV. Section V compares the proposed TCF with conventional TSFs. Conclusions form section VI.

II. Proposed Off-line TCF

The proposed TCF for commutation ripple reduction is based on generating a flux linkage profile that fully utilizes the available dc link voltage at both turn-on and turn-off. This flux profile is transformed into a current profile stored in a look-up table (LUT). Fig. 1 shows the block diagram of the proposed TCF.

A four-phase, 8/6 SRM, with specifications in Table I, is used to demonstrate the proposed TCF. The rotor pole pitch and the phase shift for an 8/6 SRM are 60º and 15º, respectively. For the SRM under study, the unaligned position is at 30^0, while the aligned position is at 60º (negative torque 0 to 30º, positive torque 30º to 60º). All the angles are given in mechanical degrees.

The SRM is driven by a conventional asymmetric half-bridge with two switches and two diodes per phase, where the three possible phase voltages are $\pm V_{dc}$ and 0V.

TABLE I
Specifications of SRM (4 kW at 1500 rpm)

Parameter	Value	Parameter	Value
No. of motor phases m	4	Rotor outer radius	45 mm
Stator/rotor poles N_s/N_r	8/6	Thickness of rotor yoke	15 mm
stator pole arc/ pole pitch	0.42	Motor axial length	155 mm
rotor pole arc/pole pitch	0.35	Length of air gap	1 mm
Turns per pole N	90	Stator inner radius	46 mm
DC link voltage V_{dc}	415 V	Stator outer radius	83 mm
Phase resistance R	0.8 Ω	Thickness of stator yoke	12 mm
Rated current	12.6 A	Shaft radius	15 mm

One or two phases (simultaneously) conduct to generate the required torque. The conduction period for each phase is limited to a maximum of 30º to avoid operation in the negative torque production region. Fig. 2 shows the phase torques and total torque for an arbitrary conduction period, $15° < \{\theta_b - \theta_a\} \leq 30°$.

In regions I and III, two phases overlap and produce additively the demand torque. While in region II, only one phase produces the required torque. If the conduction period is 30º (that is, $\theta_a = 30°$ and $\theta_b = 60°$), the second region (region II) vanishes, and only regions I and III exist.

The goal is to generate a phase torque profile, which fully utilizes the available dc link voltage and, in so doing, will offer the widest zero TR speed range. The phase torque profile will be composed of five parts. To illustrate the concept, a numerical example is given with $\theta_a = 35°$ and $\theta_b = 55°$.

When the incoming phase is at 35°, the full positive dc link voltage $+V_{dc}$ is applied (continuously - no switching) to this phase for rapid current, and hence torque, build up, in portion 1. (In this case, the incoming phase is termed the master phase). Simultaneously, the outgoing phase is at 50° (due to a 15° phase shift). The outgoing phase generates the rest of the torque so that the torque demand level is reached, portion 2 (in this case, the outgoing phase is termed the control phase). Thus, the torque profile forming the two portions 1 and 2 are known.

When angle θ_x is reached, the outgoing phase takes precedence. Hence the outgoing phase becomes the master phase, and full negative dc link voltage $-V_{dc}$, portion 3, is applied (continuously – no switching) for rapid current extinction. Simultaneously, the incoming phase becomes the control phase, portion 4, supplying the torque deficiency to maintain the torque demand. Thus, the torque portions 3 and 4 are known. Finally, portion 5, region II, is when only one phase conducts to generate the demanded torque.

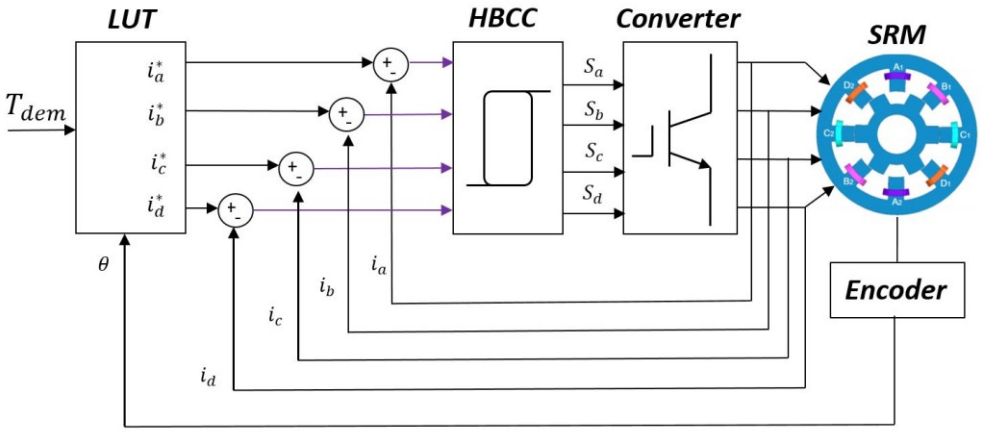

Fig. 1 Block diagram of the proposed TCF.

Concatenating the five portions, the phase torque profile is obtained. Table II demonstrates this process in the overlap region (the single-phase conduction region, portion 5, is excluded).

Table II ILLUSTRATION OF PROPOSED TCF DURING OVERLAP

Phase	Angle		Voltage	
Incoming	35°→ 35°+θ_x	35°+θ_x → 40°	Fix (+V_{dc})	Variable
Outgoing	50°→ 50°+ θ_x	50°+ θ_x → 55°	Variable	Fix (−V_{dc})

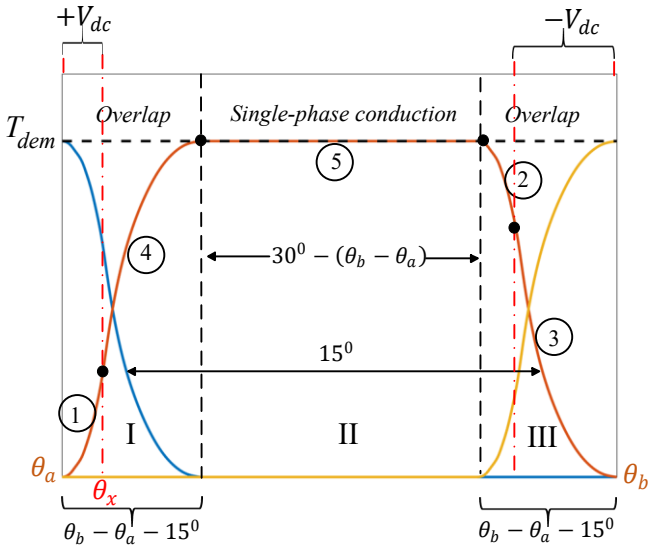

Fig. 2 Illustration of the proposed TCF.

The final step is to calculate the value of θ_x^0 which maximizes the zero TR speed ω_n (rpm).

Equation (1) defines the voltage equation at turn on/off for one SRM phase, neglecting phase winding resistance.

$$\pm V_{dc} = {}^{d\lambda}/_{dt} \tag{1}$$

where λ is the flux linkage. $+V_{dc}$ is applied (continuously) at phase turn-on (portion 1), while $-V_{dc}$ is applied (continuously) at phase turn-off (portion 3). Integrating (1) yields

$$(\lambda_f - \lambda_i) = \pm V_{dc} t \tag{2}$$

where λ_f, λ_i are the final and initial values of flux linkage, respectively, and t is time. At phase turn-on, the initial flux linkage of the phase winding is zero. Hence the final flux linkage is calculated by:

$$(\lambda_f)_{in} = \frac{+V_{dc}(\theta_x^0 - \theta_a^0)}{6\omega_n}. \tag{3}$$

At phase turn-off, the flux linkage must decay to zero at the aligned position. Hence, the final flux linkage is zero, and the initial flux linkage is calculated from

$$(-\lambda_i)_{out} = \frac{-V_{dc}(\theta_b^0 - 15^0 - \theta_x^0)}{6\omega_n}. \tag{4}$$

Equations (3) and (4) are solved iteratively to calculate θ_x^0 and ω_n ensuring that (5) is satisfied.

$$T_{dem} = T\left\{(\lambda_f)_{in}, (\theta_x)\right\} + T\{(\lambda_i)_{out}, (15^0 + \theta_x)\} \tag{5}$$

where T_{dem} is the demand torque. For the numerical example with a demand torque of 25 Nm, the angle θ_x^0 is 36.65°, ω_n is 355 rpm, $(\lambda_f)_{in}$ is 0.32 Wb-t and $(\lambda_i)_{out}$ is 0.65 Wb-t. The developed phase torques for the incoming and outgoing phases are 10.35 Nm and 14.65 Nm, respectively, and the rms phase current is 11.63 A.

III. ZERO TR SPEED RANGE OF THE PROPOSED TCF

This section investigates the maximum torque ripple-free speed range achieved at different torque demands using the proposed TCF. The maximum speed range with zero TR is calculated for 25%, 50%, 75%, and 100% full load torque (FLT).

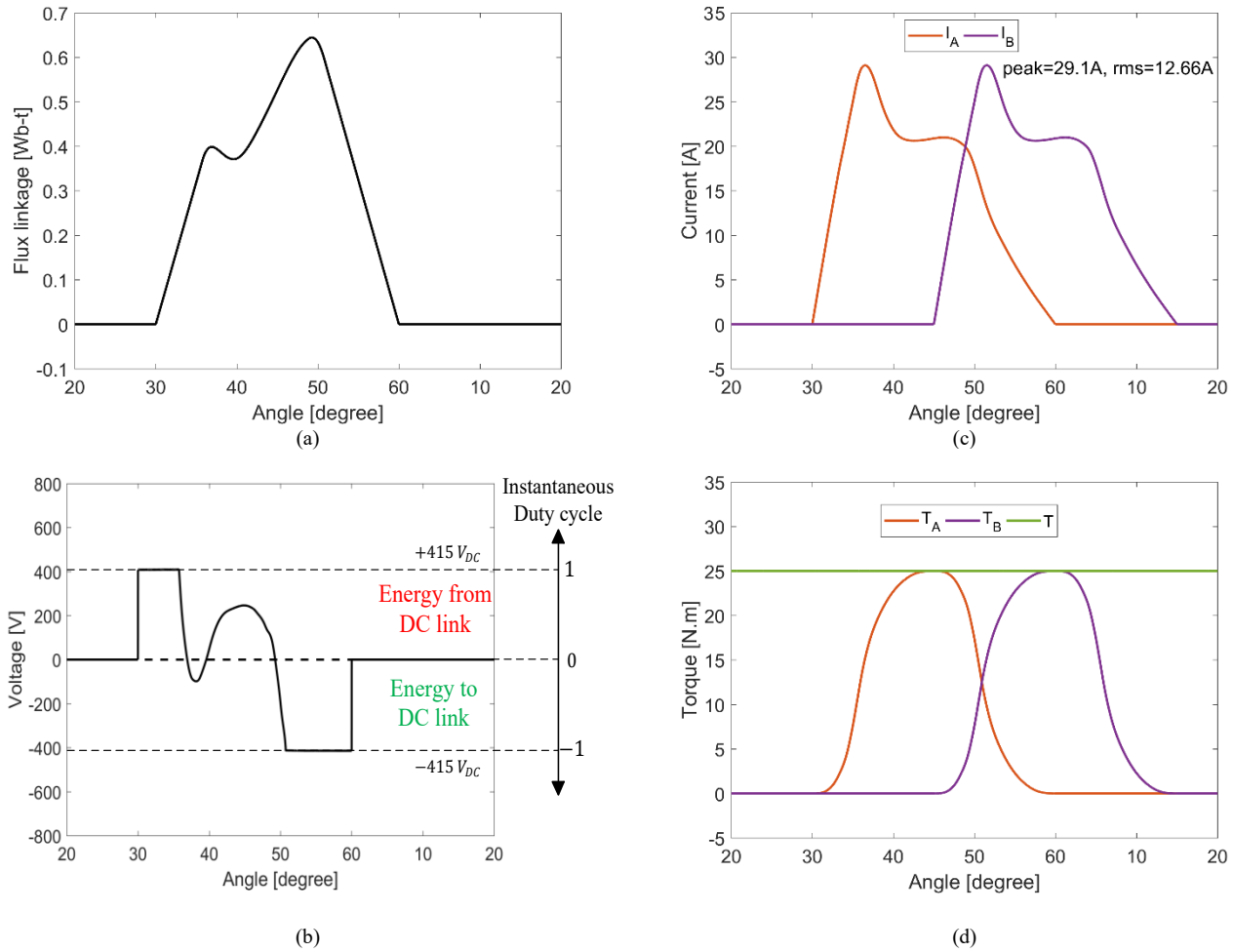

Fig. 3 SRM performance at FLT and 1065 rpm using proposed TCF (Current source model).
(a) Flux linkage waveform, (b) Rate of change of flux linkage (voltage demand), (c) Current waveforms, and (d) Torque waveforms.

The maximum conduction period for each phase is 30°. The corresponding maximum ripple-free speed at FLT is 1065 rpm. SRM performance is illustrated in Fig. 3. The flux linkage profile is shown in Fig. 3a, which is linear near the unaligned and aligned positions. This is expected as the full dc link voltage, either positive or negative, is applied (continuously) on the phase winding at turn-on and turn-off, respectively, as highlighted in Fig. 3b. The required current profiles are demonstrated in Fig. 3c. Finally, torque waveforms are plotted in Fig. 3d which shows zero TR operation.

The maximum speed, rms, and peak currents are calculated for different torque demands, namely; 25%, 50%, and 75% FLT. The results (including FLT) are summarized in Table III.

Table III TCF PERFORMANCE AT DIFFERENT TORQUE DEMANDS

T_{dem} (% FLT)	100%	75%	50%	25%
ω_n (rpm)	1065	1210	1455	2045
I_{rms} (A)	12.66	10.79	8.75	6.18
I_{peak} (A)	29.1	24.8	20	14.25

The proposed TCF extends the zero TR speed range at different torque demands. With an FLT base speed of 1500rpm, a zero torque zero ripple FLT at 1065 rpm means that 71% of the FLT speed range can be torque ripple free.

IV. SIMULATION RESULTS

In the previous sections, a TCF was proposed, which eliminates TR during phase commutation. The results were produced using an ideal current source (no semiconductor switching), where the source terminal voltage indicates the switch state duty cycle. However, when tracking the generated current profiles (that produce zero commutation torque ripple) with a voltage source converter, another form of TR appears due to switching, which produces current ripple (whence torque ripple will be termed switching TR_{sw}, as opposed to commutation torque ripple TR_{com}).

This section investigates SRM dynamic performance using the proposed TCF, and the effect of voltage switching (current ripple) on the generated TR is discussed.

The current is sampled at 200 kHz, and the hysteresis band is 0.3 A (specification parameters well within the bounds of flux gate current measurement technology). Results of the proposed TCF are presented at FLT and 1065 rpm, as illustrated in Fig. 4.

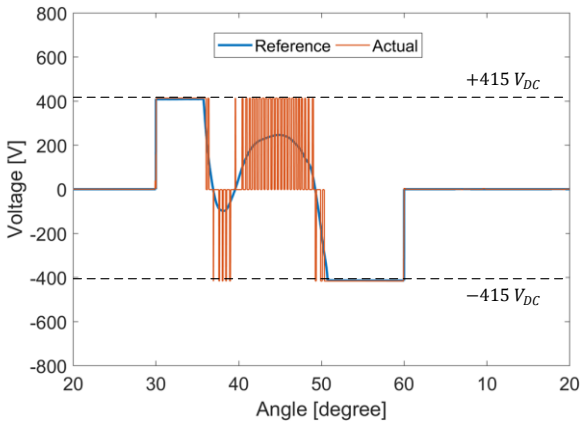

(a)

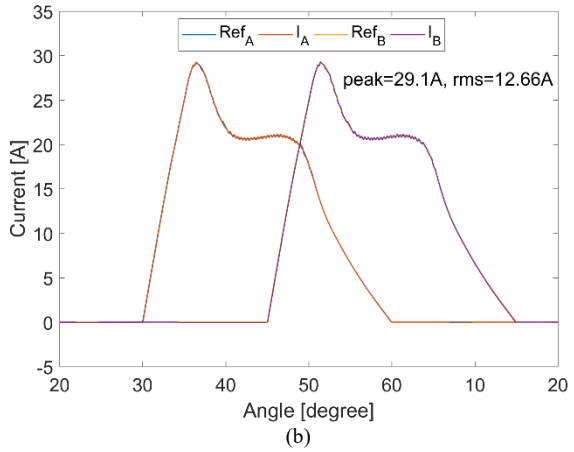

(b)

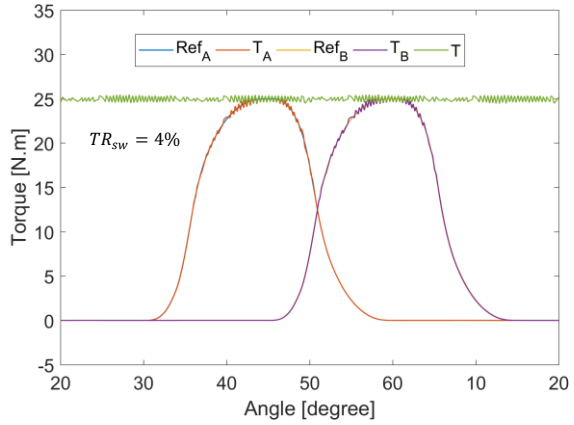

(c)

Fig. 4 SRM performance at FLT and 1065rpm using the proposed TCF.
(a) Rate of change of flux linkage (voltage demand), (b) Current waveforms, and (c) Torque waveforms.

The phase conduction period is 30°. The rate of change of flux linkage (voltage demand) is demonstrated in Fig. 4a, along with the actual phase voltage. During turn-on and turn-off, there is no switching since the voltage is in either of the continuous $\pm V_{dc}$ modes. Hence, the switching ripple is zero, and advantageously, no switching losses occur. Prior knowledge of the required voltage demand allowed using soft switching control (0V loops). When the voltage demand is positive, and both switches have periods simultaneously on ($+V_{dc}$), the switches are alternately turned off to alternate the zero-volt loops. When the voltage demand is negative, and both switches have periods of being simultaneously off ($-V_{dc}$), each switch is alternately turned on to create alternating zero-volt loops. This alternating 0V loop method balances the switching losses, and halves switch switching frequency.

Fig. 4b shows actual and reference phase currents showing excellent tracking at the unaligned and aligned positions.

The phase torques, along with the total developed torque, are illustrated in Fig. 4c. A 4% torque ripple TR_{sw} due to switching is recorded. This is the sole torque ripple here, as the torque ripple TR_{com} due to commutation is completely eliminated. Given that the Nm/A is high in the switching region, only an increase in switching frequency (narrower hysteresis band) can reduce the TR. Using a 0.1 A hysteresis band reduces the switching TR_{sw} from 4% to 2%.

V. Comparison between proposed TCF and conventional TSFs

This section presents a comparison between the proposed TCF and conventional TSF. As the Cos TSF method produces the best performance (it accounts for the SRM non-linearity as opposed to linear TSF), it is taken as a reference for comparison.

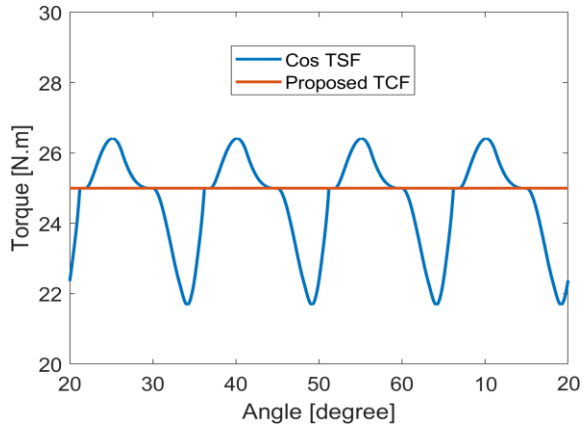

(a)

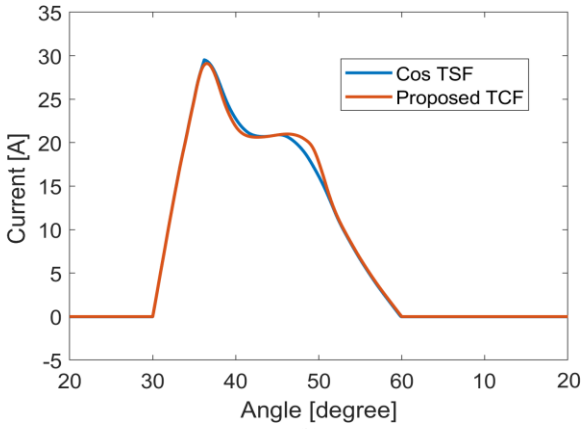

(b)

Fig. 5 Comparison of SRM performance at FLT and 1065rpm using the proposed TCF against the Cos TSF method.
(a) Torque waveforms, and (b) Current waveforms.

Since the paper aims to investigate the ripple-free speed range of the SRM (i.e., minimization of commutation TR), therefore, the comparison presented in this section is carried out at high switching frequency to attenuate the effect of switching TR (which is inevitable in any TR minimization approach), leaving only the TR due to commutation. This will highlight the advantages of the proposed TCF compared to the conventional Cos TSF method.

Fig. 5 compares the performance of the proposed TCF against the Cos TSF at FLT and 1065rpm with 30º conduction period (i.e., for Cos TSF turn on is at an unaligned position, while turn off is adjusted to result in actual current extinguishing at an aligned position), where torque waveforms are demonstrated in Fig. 5a showing smooth ripple-free torque waveform using the proposed TCF. Conversely, at the same speed and FLT, the Cos TSF method produces 20% TR solely due to commutation.

Fig. 5b shows the phase current profiles for both approaches, where the proposed TCF produces current values of 12.66A rms with 29.1 A peak against 12.61 A rms and 29.5 A peak for the Cos TSF method. Results are close and within the current rating of the SRM under study.

VI. Conclusion

A new TCF has been proposed and investigated, which exploits maximum utilization of the dc link voltage at phase turn-on and turn-off. This extends the zero TR speed range significantly. This TCF is adaptable to any SRM with any number of phases (≥3) and stator/rotor pole number. Only magnetic characteristics (either obtained using FEA or experimentally) are needed. The SRM maximum speed range with theoretically zero TR was determined. The proposed TCF is characterized by low switching losses, as switching is required only for a conduction period equal to the stroke angle. In addition, soft switching is used as opposed to conventional TSFs that require either hard or at least hybrid switching. The proposed TCF was tested on a four-phase, 8/6 SRM, where ripple-free operation was possible up to 71% of the base speed. Theoretical results were validated by simulation.

Acknowledgment

The presented research was supported by EPSRC Grant EP/R029504/1.

References

[1] K. Rahman, B. Fahimi, G. Suresh, A. Rajarathnam, and M. Ehsani, “Advantages of switched reluctance motor applications to EV and HEV: design and control issues,” *IEEE Trans. Ind. Appl.*, vol. 36, no. 1, pp. 111-121, Jan.-Feb. 2000.

[2] S. Wang, Q. Zhan, Z. Ma, and L. Zhou, “Implementation of a 50-kW four-phase switched reluctance motor drive system for hybrid electric vehicle," *IEEE Trans. Magn.*, vol. 41, no. 1, pp. 501-504, Jan. 2005.

[3] H. Makino, T. Kosaka, and N. Matsui, “Digital PWM-control-based active vibration cancellation for switched reluctance motors,” *IEEE Trans. Ind. Appl.*, vol. 51, no. 6, pp. 175-182, Dec. 2015.

[4] E. Bostanci, M. Moallem, A. Parsapour, and B. Fahimi, “Opportunities and challenges of switched reluctance motor drives for electric propulsion: a comparative study,” *IEEE Trans. Transport. Electrific.*, vol. 3, no. 1, pp. 58-75, Mar. 2017.

[5] A. Abdel-Aziz, K. Ahmed, S. Wang, A. Massoud, and B. Williams, “A neutral-point diode-clamped converter with inherent voltage-boosting for a four-phase SRM Drive,” *IEEE Trans. Ind. Electron.*, vol. 67, no. 7, pp. 5313-5324, Jul. 2020.

[6] P. Ramesh and N. C. Lenin, “High power density electrical machines for electric vehicles—comprehensive review based on material technology," *IEEE Trans. Magn.*, vol. 55, no. 11, pp. 1-21, Nov. 2019.

[7] N. Saha, A. Panda, and S. Panda, “Speed control with torque ripple reduction of switched reluctance motor by many optimizing liaison technique,” *J. Electrical Syst. Inform. Technology*, vol. 5, no. 5, pp. 829-842, 2018.

[8] Gan, Q. Sun, W. Kong, H. Li, and Y. Hu, “A review on machine topologies and control techniques for low-noise switched reluctance motors in electric vehicle applications,’’ *IEEE Access*, vol. 6 pp. 31430-31443, 2018.

[9] G. Fang, F. Scalcon, D. Xiao, R. Vieira, H. Gründling, and A. Emadi, “Advanced control of switched reluctance motors (SRMs): a review on current regulation, torque control, and vibration suppression,” *IEEE Open J. Ind. Electron. Soc.*, vol. 2, pp. 280-301, 2021.

[10] T. Husain, A. Elrayyah, Y. Sozer, and I. Husain, “Unified control for switched reluctance motors for wide speed operation,” *IEEE Trans. Ind. Electron.*, vol. 66, no. 5, pp. 3401-3411, May 2019.

[11] X. Zhang, Q. Yang, M. Ma, Z. Lin, and S. Yang, “A switched reluctance motor torque ripple reduction strategy with deadbeat current control and active thermal management,” *IEEE Trans. Veh. Technology*, vol. 69, no. 1, pp. 317-327, Jan. 2020.

[12] V. Vujičić, “Minimization of torque ripple and copper losses in switched reluctance drive,” *IEEE Trans. Power Electron.*, vol. 27, no. 1, pp. 388-399, Jan. 2012.

[13] X. Xue, K. Cheng, and S. Ho, “Optimization and evaluation of torque-sharing functions for torque ripple minimization in switched reluctance motor drives,” *IEEE Trans. Power Electron.*, vol. 24, no. 9, pp. 2076-2090, Sep. 2009.

[14] D. Lee, J. Liang, Z. Lee, and J. Ahn, “A simple nonlinear logical torque sharing function for low-torque ripple SR drive,” *IEEE Trans. Ind. Electron.*, vol. 56, no. 8, pp. 3021-3028, Aug. 2009.

[15] J. Ye, B. Bilgin, and A. Emadi, “An extended-speed low-ripple torque control of switched reluctance motor drives,” *IEEE Trans. Power Electron.*, vol. 30, no. 3, pp. 1457-1470, Mar. 2015.

[16] J. Ye, B. Bilgin, and A. Emadi, “An offline torque sharing function for torque ripple reduction in switched reluctance motor drives,” *IEEE Trans. Energy Conversion*, vol. 30, no. 2, pp. 726-735, Jun. 2015.

[17] Gan, J. Wu, Q. Sun, S. Yang, Y. Hu, and L. Jin, “Low-cost direct instantaneous torque control for switched reluctance motors with bus current detection under soft-chopping mode,” *IET Power Electron.*, vol. 9, no. 3, pp. 482-490, 9 3 2016.

[18] Q. Sun, J. Wu, C. Gan, Y. Hu, and J. Si, “OCTSF for torque ripple minimization in SRMs,” *IET Power Electron.*, vol. 9, no. 14, pp. 2741-2750, 16 11 2016.

[19] H. Li, B. Bilgin, and A. Emadi, “An improved torque sharing function for torque ripple reduction in switched reluctance machines,” *IEEE Trans. Power Electron.*, vol. 34, no. 2, pp. 1635-1644, Feb. 2019.

[20] A. K. Rana and A. V. R. Teja, “A mathematical torque ripple minimization technique based on a nonlinear modulating factor for switched reluctance motor drives,” *IEEE Trans. Ind. Electron.*, vol. 69, no. 2, pp. 1356-1366, Feb. 2022.